2023-2024

THÈSE

pour le

DIPLÔME D'ÉTAT DE DOCTEUR EN MÉDECINE

Qualification en RADIODIAGNOSTIC ET IMAGERIE MEDICALE

EVALUATION OF WASHOUT USING IMAGE SUBTRACTION FOR THE DIAGNOSIS OF HEPATOCELLULAR CARCINOMA IN CIRRHOTIC PATIENTS WITH NATIVE T1-HYPERINTENSE NODULES

EVALUATION DU LAVAGE EN IRM AVEC SOUSTRACTION DANS LE DIAGNOSTIC DE CARCINOME HÉPATOCELLULAIRE PARMI LES NODULES EN HYPERSIGNAL T1 SPONTANÉ CHEZ LES PATIENTS CIRRHOTIQUES

BIZEUL Jocelyn

Né le 07/02/1996 à Angers France

Sous la direction du Dr PAISANT Anita

Membres du jury

Monsieur le Professeur AUBE Christophe	Président
Madame le Docteur PAISANT Anita	Directrice
Monsieur le Professeur BOURSIER Jérôme	Membre
Monsieur le Docteur LEBIGOT Jérôme	Membre
Madame le Docteur CANIVET Clémence	Membre

Soutenue publiquement le :
27 septembre 2023

FACULTÉ DE SANTÉ
UNIVERSITÉ D'ANGERS

ENGAGEMENT DE NON PLAGIAT

Je, soussigné BIZEUL Jocelyn
déclare être pleinement conscient que le plagiat de documents ou d'une partie d'un document publiée sur toutes formes de support, y compris l'internet, constitue une violation des droits d'auteur ainsi qu'une fraude caractérisée.
En conséquence, je m'engage à citer toutes les sources que j'ai utilisées pour écrire ce rapport ou mémoire.

signé par l'étudiant le **24/07/2023**

SERMENT D'HIPPOCRATE

« Au moment d'être admis(e) à exercer la médecine, je promets et je jure d'être fidèle aux lois de l'honneur et de la probité. Mon premier souci sera de rétablir, de préserver ou de promouvoir la santé dans tous ses éléments, physiques et mentaux, individuels et sociaux. Je respecterai toutes les personnes, leur autonomie et leur volonté, sans aucune discrimination selon leur état ou leurs convictions. J'interviendrai pour les protéger si elles sont affaiblies, vulnérables ou menacées dans leur intégrité ou leur dignité. Même sous la contrainte, je ne ferai pas usage de mes connaissances contre les lois de l'humanité. J'informerai les patients des décisions envisagées, de leurs raisons et de leurs conséquences. Je ne tromperai jamais leur confiance et n'exploiterai pas le pouvoir hérité des circonstances pour forcer les consciences. Je donnerai mes soins à l'indigent et à quiconque me les demandera. Je ne me laisserai pas influencer par la soif du gain ou la recherche de la gloire.

Admis(e) dans l'intimité des personnes, je tairai les secrets qui me seront confiés. Reçu (e) à l'intérieur des maisons, je respecterai les secrets des foyers et ma conduite ne servira pas à corrompre les mœurs. Je ferai tout pour soulager les souffrances. Je ne prolongerai pas abusivement les agonies. Je ne provoquerai jamais la mort délibérément.

Je préserverai l'indépendance nécessaire à l'accomplissement de ma mission. Je n'entreprendrai rien qui dépasse mes compétences. Je les entretiendrai et les perfectionnerai pour assurer au mieux les services qui me seront demandés.

J'apporterai mon aide à mes confrères ainsi qu'à leurs familles dans l'adversité. Que les hommes et mes confrères m'accordent leur estime si je suis fidèle à mes promesses ; que je sois déshonoré (e) et méprisé(e) si j'y manque ».

LISTE DES ENSEIGNANTS DE LA FACULTÉ DE SANTÉ D'ANGERS

Doyen de la Faculté : Pr Nicolas Lerolle
Vice-Doyen de la Faculté et directeur du département de pharmacie : Pr Frédéric Lagarce
Directeur du département de médecine : Pr Cédric Annweiler

PROFESSEURS DES UNIVERSITÉS

ABRAHAM Pierre	PHYSIOLOGIE	Médecine
ANGOULVANT Cécile	MEDECINE GENERALE	Médecine
ANNWEILER Cédric	GERIATRIE ET BIOLOGIE DU VIEILLISSEMENT	Médecine
ASFAR Pierre	REANIMATION	Médecine
AUBE Christophe	RADIOLOGIE ET IMAGERIE MEDICALE	Médecine
AUGUSTO Jean-François	NEPHROLOGIE	Médecine
BAUFRETON Christophe	CHIRURGIE THORACIQUE ET CARDIOVASCULAIRE	Médecine
BELLANGER William	MEDECINE GENERALE	Médecine
BENOIT Jean-Pierre	PHARMACOTECHNIE	Pharmacie
BIERE Loïc	CARDIOLOGIE	Médecine
BIGOT Pierre	UROLOGIE	Médecine
BONNEAU Dominique	GENETIQUE	Médecine
BOUCHARA Jean-Philippe	PARASITOLOGIE ET MYCOLOGIE	Médecine
BOUET Pierre-Emmanuel	GYNECOLOGIE-OBSTETRIQUE	Médecine
BOURSIER Jérôme	GASTROENTEROLOGIE ; HEPATOLOGIE	Médecine
BOUVARD Béatrice	RHUMATOLOGIE	
BRIET Marie	PHARMACOLOGIE	Médecine
CALES Paul	GASTROENTEROLOGIE ; HEPATOLOGIE	Médecine
CAMPONE Mario	CANCEROLOGIE ; RADIOTHERAPIE	Médecine
CAROLI-BOSC François-Xavier	GASTROENTEROLOGIE ; HEPATOLOGIE	Médecine
CASSEREAU Julien	NEUROLOGIE	Médecine
CONNAN Laurent	MEDECINE GENERALE	Médecine

COPIN Marie-Christine	ANATOMIE ET CYTOLOGIE PATHOLOGIQUES	Médecine
COUTANT Régis	PEDIATRIE	Médecine
CUSTAUD Marc-Antoine	PHYSIOLOGIE	Médecine
CRAUSTE-MANCIET Sylvie	PHARMACOTECHNIE HOSPITALIERE	Pharmacie
DE CASABIANCA Catherine	MEDECINE GENERALE	Médecine
DESCAMPS Philippe	GYNECOLOGIE-OBSTETRIQUE	Médecine
D'ESCATHA Alexis	MEDECINE ET SANTE AU TRAVAIL	Médecine
DINOMAIS Mickaël	MEDECINE PHYSIQUE ET DE READAPTATION	Médecine
DUBEE Vincent	MALADIES INFECTIEUSES ET TROPICALES	Médecine
DUCANCELLE Alexandra	BACTERIOLOGIE-VIROLOGIE ; HYGIENE HOSPITALIERE	Médecine
DUVAL Olivier	CHIMIE THERAPEUTIQUE	Pharmacie
DUVERGER Philippe	PEDOPSYCHIATRIE	Médecine
EVEILLARD Mathieu	BACTERIOLOGIE-VIROLOGIE	Pharmacie
FAURE Sébastien	PHARMACOLOGIE PHYSIOLOGIE	Pharmacie
FOURNIER Henri-Dominique	ANATOMIE	Médecine
FOUQUET Olivier	CHIRURGIE THORACIQUE ET CARDIOVASCULAIRE	Médecine
FURBER Alain	CARDIOLOGIE	Médecine
GAGNADOUX Frédéric	PNEUMOLOGIE	Médecine
GOHIER Bénédicte	PSYCHIATRIE D'ADULTES	Médecine
GUARDIOLA Philippe	HEMATOLOGIE ; TRANSFUSION	Médecine
GUILET David	CHIMIE ANALYTIQUE	Pharmacie
HAMY Antoine	CHIRURGIE GENERALE	Médecine
HENNI Samir	MEDECINE VASCULAIRE	Médecine
HUNAULT-BERGER Mathilde	HEMATOLOGIE ; TRANSFUSION	Médecine
IFRAH Norbert	HEMATOLOGIE ; TRANSFUSION	Médecine
JEANNIN Pascale	IMMUNOLOGIE	Médecine
KEMPF Marie	BACTERIOLOGIE-VIROLOGIE ; HYGIENE HOSPITALIERE	Médecine
KUN-DARBOIS Daniel	CHIRURGIE MAXILLO-FACIALE ET STOMATOLOGIE	Médecine
LACOEUILLE FRANCK	RADIOPHARMACIE	Pharmacie

LACCOURREYE Laurent	OTO-RHINO-LARYNGOLOGIE	Médecine
LAGARCE Frédéric	BIOPHARMACIE	Pharmacie
LARCHER Gérald	BIOCHIMIE ET BIOLOGIE MOLECULAIRES	Pharmacie
LASOCKI Sigismond	ANESTHESIOLOGIE-REANIMATION	Médecine
LEBDAI Souhil	UROLOGIE	Médecine
LEGENDRE Guillaume	GYNECOLOGIE-OBSTETRIQUE	Médecine
LEGRAND Erick	RHUMATOLOGIE	Médecine
LERMITE Emilie	CHIRURGIE GENERALE	Médecine
LEROLLE Nicolas	REANIMATION	Médecine
LUNEL-FABIANI Françoise	BACTERIOLOGIE-VIROLOGIE ; HYGIENE HOSPITALIERE	Médecine
MARCHAIS Véronique	BACTERIOLOGIE-VIROLOGIE	Pharmacie
MARTIN Ludovic	DERMATO-VENEREOLOGIE	Médecine
MAY-PANLOUP Pascale	BIOLOGIE ET MEDECINE DU DEVELOPPEMENT ET DE LA REPRODUCTION	Médecine
MENEI Philippe	NEUROCHIRURGIE	Médecine
MERCAT Alain	REANIMATION	Médecine
PAPON Nicolas	PARASITOLOGIE ET MYCOLOGIE MEDICALE	Pharmacie
PASSIRANI Catherine	CHIMIE GENERALE	Pharmacie
PELLIER Isabelle	PEDIATRIE	Médecine
PETIT Audrey	MEDECINE ET SANTE AU TRAVAIL	Médecine
PICQUET Jean	CHIRURGIE VASCULAIRE ; MEDECINE VASCULAIRE	Médecine
PODEVIN Guillaume	CHIRURGIE INFANTILE	Médecine
PROCACCIO Vincent	GENETIQUE	Médecine
PRUNIER Delphine	BIOCHIMIE ET BIOLOGIE MOLECULAIRE	Médecine
PRUNIER Fabrice	CARDIOLOGIE	Médecine
RAMOND-ROQUIN Aline	MEDECINE GENERALE	Médecine
REYNIER Pascal	BIOCHIMIE ET BIOLOGIE MOLECULAIRE	Médecine
RICHARD Isabelle	MEDECINE PHYSIQUE ET DE READAPTATION	Médecine
RICHOMME Pascal	PHARMACOGNOSIE	Pharmacie
RODIEN Patrice	ENDOCRINOLOGIE, DIABETE ET MALADIES METABOLIQUES	Médecine

ROQUELAURE Yves	MEDECINE ET SANTE AU TRAVAIL	Médecine
ROUGE-MAILLART Clotilde	MEDECINE LEGALE ET DROIT DE LA SANTE	Médecine
ROUSSEAU Audrey	ANATOMIE ET CYTOLOGIE PATHOLOGIQUES	Médecine
ROUSSEAU Pascal	CHIRURGIE PLASTIQUE, RECONSTRUCTRICE ET ESTHETIQUE	Médecine
ROUSSELET Marie-Christine	ANATOMIE ET CYTOLOGIE PATHOLOGIQUES	Médecine
ROY Pierre-Marie	MEDECINE D'URGENCE	Médecine
SAULNIER Patrick	BIOPHYSIQUE ET BIOSTATISTIQUES	Pharmacie
SERAPHIN Denis	CHIMIE ORGANIQUE	Pharmacie
SCHMIDT Aline	HEMATOLOGIE ; TRANSFUSION	Médecine
TESSIER-CAZENEUVE Christine	MEDECINE GENERALE	Médecine
TRZEPIZUR Wojciech	PNEUMOLOGIE	Médecine
UGO Valérie	HEMATOLOGIE ; TRANSFUSION	Médecine
URBAN Thierry	PNEUMOLOGIE	Médecine
VAN BOGAERT Patrick	PEDIATRIE	Médecine
VENARA Aurélien	CHIRURGIE VISCERALE ET DIGESTIVE	Médecine
VENIER-JULIENNE Marie-Claire	PHARMACOTECHNIE	Pharmacie
VERNY Christophe	NEUROLOGIE	Médecine
WILLOTEAUX Serge	RADIOLOGIE ET IMAGERIE MEDICALE	Médecine

MAÎTRES DE CONFÉRENCES

BAGLIN Isabelle	CHIMIE THERAPEUTIQUE	Pharmacie
BASTIAT Guillaume	BIOPHYSIQUE ET BIOSTATISTIQUES	Pharmacie
BEAUVILLAIN Céline	IMMUNOLOGIE	Médecine
BEGUE Cyril	MEDECINE GENERALE	Médecine
BELIZNA Cristina	MEDECINE INTERNE	Médecine
BELONCLE François	REANIMATION	Médecine
BENOIT Jacqueline	PHARMACOLOGIE	Pharmacie
BESSAGUET Flavien	PHYSIOLOGIE PHARMACOLOGIE	Pharmacie
BERNARD Florian	ANATOMIE ; discipline hospit : NEUROCHIRURGIE	Médecine
BLANCHET Odile	HEMATOLOGIE ; TRANSFUSION	Médecine
BOISARD Séverine	CHIMIE ANALYTIQUE	Pharmacie
BRIET Claire	ENDOCRINOLOGIE, DIABETE ET MALADIES METABOLIQUES	Médecine

BRIS Céline	BIOCHIMIE ET BIOLOGIE MOLECULAIRE	Pharmacie
CAPITAIN Olivier	CANCEROLOGIE ; RADIOTHERAPIE	Médecine
CHAO DE LA BARCA Juan-Manuel	BIOCHIMIE ET BIOLOGIE MOLECULAIRE	Médecine
CHEVALIER Sylvie	BIOLOGIE CELLULAIRE	Médecine
CLERE Nicolas	PHARMACOLOGIE / PHYSIOLOGIE	Pharmacie
COLIN Estelle	GENETIQUE	Médecine
DERBRE Séverine	PHARMACOGNOSIE	Pharmacie
DESHAYES Caroline	BACTERIOLOGIE VIROLOGIE	Pharmacie
DOUILLET Delphine	MEDECINE D'URGENCE	Médecine
FERRE Marc	BIOLOGIE MOLECULAIRE	Médecine
FORTRAT Jacques-Olivier	PHYSIOLOGIE	Médecine
GUELFF Jessica	MEDECINE GENERALE	Médecine
HAMEL Jean-François	BIOSTATISTIQUES, INFORMATIQUE MEDICALE	Médicale
HELESBEUX Jean-Jacques	CHIMIE ORGANIQUE	Pharmacie
HERIVAUX Anaïs	BIOTECHNOLOGIE	Pharmacie
HINDRE François	BIOPHYSIQUE	Médecine
JOUSSET-THULLIER Nathalie	MEDECINE LEGALE ET DROIT DE LA SANTE	Médecine
JUDALET-ILLAND Ghislaine	MEDECINE GENERALE	Médecine
KHIATI Salim	BIOCHIMIE ET BIOLOGIE MOLECULAIRE	Médecine
LANDREAU Anne	BOTANIQUE/ MYCOLOGIE	Pharmacie
LEGEAY Samuel	PHARMACOCINETIQUE	Pharmacie
LEMEE Jean-Michel	NEUROCHIRURGIE	Médecine
LE RAY-RICHOMME Anne-Marie	PHARMACOGNOSIE	Pharmacie
LEPELTIER Elise	CHIMIE GENERALE	Pharmacie
LETOURNEL Franck	BIOLOGIE CELLULAIRE	Médecine
LIBOUBAN Hélène	HISTOLOGIE	Médecine
LUQUE PAZ Damien	HEMATOLOGIE BIOLOGIQUE	Médecine
MABILLEAU Guillaume	HISTOLOGIE, EMBRYOLOGIE ET CYTOGENETIQUE	Médecine
MALLET Sabine	CHIMIE ANALYTIQUE	Pharmacie
MAROT Agnès	PARASITOLOGIE ET MYCOLOGIE MEDICALE	Pharmacie
MESLIER Nicole	PHYSIOLOGIE	Médecine
MIOT Charline	IMMUNOLOGIE	Médecine
MOUILLIE Jean-Marc	PHILOSOPHIE	Médecine

NAIL BILLAUD Sandrine	IMMUNOLOGIE	Pharmacie
PAILHORIES Hélène	BACTERIOLOGIE-VIROLOGIE	Médecine
PAPON Xavier	ANATOMIE	Médecine
PASCO-PAPON Anne	RADIOLOGIE ET IMAGERIE MEDICALE	Médecine
PECH Brigitte	PHARMACOTECHNIE	Pharmacie
PENCHAUD Anne-Laurence	SOCIOLOGIE	Médecine
PIHET Marc	PARASITOLOGIE ET MYCOLOGIE	Médecine
POIROUX Laurent	SCIENCES INFIRMIERES	Médecine
PY Thibaut	MEDECINE GENERALE	Médecine
RINEAU Emmanuel	ANESTHESIOLOGIE REANIMATION	Médecine
RIOU Jérémie	BIOSTATISTIQUES	Pharmacie
RIQUIN Elise	PEDOPSYCHIATRIE ; ADDICTOLOGIE	Médecine
RONY Louis	CHIRURGIE ORTHOPEDIQUE ET TRAUMATOLOGIQUE	Médecine
ROGER Emilie	PHARMACOTECHNIE	Pharmacie
SAVARY Camille	PHARMACOLOGIE-TOXICOLOGIE	Pharmacie
SCHMITT Françoise	CHIRURGIE INFANTILE	Médecine
SCHINKOWITZ Andréas	PHARMACOGNOSIE	Pharmacie
SPIESSER-ROBELET Laurence	PHARMACIE CLINIQUE ET EDUCATION THERAPEUTIQUE	Pharmacie
TEXIER-LEGENDRE Gaëlle	MEDECINE GENERALE	Médecine
VIAULT Guillaume	CHIMIE ORGANIQUE	Pharmacie

AUTRES ENSEIGNANTS

PRCE		
AUTRET Erwan	ANGLAIS	Santé
BARBEROUSSE Michel	INFORMATIQUE	Santé
FISBACH Martine	ANGLAIS	Santé
O'SULLIVAN Kayleigh	ANGLAIS	Santé
RIVEAU Hélène	ANGLAIS	
PAST		
CAVAILLON Pascal	PHARMACIE INDUSTRIELLE	Pharmacie
DILÉ Nathalie	OFFICINE	Pharmacie
GUILLET Anne-Françoise	PHARMACIE DEUST PREPARATEUR	Pharmacie

MOAL Frédéric	PHARMACIE CLINIQUE	Pharmacie
PAPIN-PUREN Claire	OFFICINE	Pharmacie
KAASSIS Mehdi	GASTRO-ENTEROLOGIE	Médecine
GUITTON Christophe	MEDECINE INTENSIVE-REANIMATION	Médecine
SAVARY Dominique	MEDECINE D'URGENCE	Médecine
POMMIER Pascal	CANCEROLOGIE-RADIOTHERAPIE	Médecine
PICCOLI Giorgina	NEPHROLOGIE	Médecine
PLP		
CHIKH Yamina	ECONOMIE-GESTION	Médecine

REMERCIEMENTS

A mon Jury,
A Monsieur le Professeur Christophe AUBE qui m'a fait l'honneur de présider ce jury. Je vous remercie pour l'intérêt que vous avez bien voulu porter à ce travail, pour vos conseils et ces 4 années d'apprentissage au sein de votre département d'imagerie.
A Madame le Docteur Anita PAISANT, qui m'a guidé dans ce travail. Merci pour ton encadrement, tes encouragements et tes conseils.
A Monsieur le Professeur Jérôme BOURSIER et Madame le Docteur Clémence CANIVET, qui m'ont fait l'honneur de juger ce travail. Je vous remercie pour votre expertise.
A Monsieur le Docteur Jérôme LEBIGOT, qui m'a fait l'honneur de juger ce travail. Merci pour ta pédagogie et tes conseils.

A Messieurs le Professeur Maxime RONOT et le Dr Roberto CANNELLA, à Madame Marine ROUX, qui m'ont aidé dans ce travail. Je vous remercie pour votre expertise et vos conseils.

A ma Famille,
A Pauline, mon amour. Merci de m'avoir soutenu durant ces années.
A mes parents avec qui je n'aurai jamais été jusque-là sans eux. Merci pour votre soutien durant ces années.
A mes frères.
A ma grand-mère, mes défunts grands-parents.
A mes oncles et tantes, cousins et cousines.
A nos chats Suga et Pepper.

A mes Amis et Collèges,
Au groupe Voila Voila.
A la team Déter.
Au groupe Laser Game.
A mes co-internes.
Aux radiologues du CHU, du CH du Mans, du CH de Saumur et de l'ICO, merci pour votre compagnonnage.
A Marie Bost, pour ton aide et ta réactivité.
Aux manipulateurs, secrétaires, aides techniques et agents d'entretien des services de radiologie dans lesquels j'ai travaillé.

PLAN

ABREVIATIONS

AP :	Arterial phase
APASL :	Asian Pacific Association for the Study of the Liver
APHE :	Arterial phase hyper-enhancement
DP :	Delayed phase
EASL :	European Association for the Study of the Liver
ECA :	Extracellular contrast agent
HBA :	Hepatobiliary contrast agent
HBP :	Hepatobiliary phase
HCC :	Hepatocellular carcinoma
KLCA-NCC :	Korean Liver Cancer Association-National Cancer Center
LI-RADS :	Liver Imaging Reporting and Data System
PVP :	Portal venous phase
SD :	Standard deviation
TP :	Transitional phase

EVALUATION OF WASHOUT USING IMAGE SUBTRACTION FOR THE DIAGNOSIS OF HEPATOCELLULAR CARCINOMA IN CIRRHOTIC PATIENTS WITH NATIVE T1-HYPERINTENSE NODULES

Jocelyn Bizeul [a], Maxime Ronot [b], Marine Roux [c,] Roberto Cannella[b,d,e], Jérôme Lebigot [a,c], Christophe Aubé [a,c], Anita Paisant [a,c]

[a] Department of Radiology, Angers University Hospital (Centre Hospitalier Universitaire d'Angers), 49000 Angers, France

[b] Université Paris Cité, INSERM U1149 "Center for Inflammation Research" (centre de recherche sur l'inflammation), CRI, Paris, & Service de radiologie, Hôpital Beaujon, AP-HP Nord, 92110 Clichy, France

[c] HIFIH Laboratory, UPRES 3859, SFR 4208, University of Angers, 49045 Angers, France

[d] Section of Radiology - Department of Biomedicine, Neuroscience and Advanced Diagnostics (BiND), University Hospital "Paolo Giaccone", 90127 Palermo, Italy

[e] Department of Health Promotion Sciences, Mother and Child Care, Internal Medicine and Medical Specialties, PROMISE, University of Palermo, 90127 Palermo, Italy

ABSTRACT

Purpose: The purpose of this study was to assess the value of subtraction on post-arterial phase images (*i.e.*, portal venous, delayed/transitional and hepatobiliary phases) for the non-invasive diagnosis of hepatocellular carcinoma (HCC) in spontaneously hyperintense nodules on T1-weighted imaging in patients with cirrhosis.

Materials and methods: Forty-five patients with a total 55 hepatic nodules that were spontaneously hyperintense on T1-weighted images were initially retrieved. All patients underwent MRI examination of the liver using extracellular agent. Each nodule was assessed for sensitivity and specificity using LI-RADS (Liver Imaging Reporting and Data System) during two reading sessions performed first without then with subtraction images on post-arterial phase images. The final gold standard was defined by a step-by-step algorithm previously published combining histology, typical imaging, alfa fetoprotein and follow-up.

Results: Forty-six nodules (26 HCC) in 39 patients with cirrhosis were analyzed. Using LI-RADS, the sensitivity and specificity for the diagnosis of HCC were 64% (95% CI: 41, 83) and 67% (95% CI: 41, 87) without subtraction images; and 73% (95%CI: 50, 89) (P = 1.000) and 33% (95%CI: 13, 59) (P = 0.553) on subtraction images using extracellular contrast agent. Fifty-five percent (22/40) of nodules displayed a washout without subtraction and 70% (28/40) did so on subtraction images obtained with extracellular contrast agent. Twenty nodules out of 40 (50%) were classified LI-RADS 5 without subtraction, and 28 out of 40 nodules (70%) with subtraction.

Conclusion: These results suggest that the use of subtraction images on post-arterial phase images (i.e., PVP, DP/TP and HBP) is not relevant for the non-invasive diagnosis of HCC for spontaneously hyperintense nodules on T1-weighted images in patients with liver cirrhosis.

INTRODUCTION

The diagnosis of hepatocellular carcinoma (HCC) can be made non-invasively without histopathological confirmation in high-risk patients (i.e., those with cirrhosis according to the European Association for the Study of the Liver [EASL v.2018], chronic hepatitis B viral infection, current or prior HCC according to the Liver Imaging Reporting And Data System [LI-RADS v.2018]), provided that the liver nodules display typical imaging features [1–3]. These typical imaging features slightly differ among international guidelines, but all include at least arterial phase hyper-enhancement (APHE) and washout [1–6].

The assessment of these two features is purely visual and does not rely on quantitative methods. The depiction of APHE can be challenging for nodules that are spontaneously hyperintense on T1-weighted images. The reported rate of spontaneously hyperintense nodules on T1-weighted images in cirrhotic liver, ranges from 12 to 25% of observations [7–9]. The differentials include HCCs but also regenerative or dysplastic nodules, adenoma and focal nodular hyperplasia [10]. Seventeen p. cent of HCCs can also show hyperintensity on T1-weighted images due to the accumulation of copper, iron and/or manganese. Hyperintensity on T1-weighted images is associated with the degree of differentiation, being reported for Edmonson grade 1 or 2 HCCs, but not grades 3 or 4 [11]. To address this, guidelines recommend the use of arterial phase subtraction images [12,13]. However, using such subtraction images on post-arterial phases (i.e., portal venous phase [PVP], delayed phase [DP], transitional phase [TP] and hepatobiliary phase [HBP]) to extract features, especially washout, has never been properly investigated and is not currently included in international recommendations.

The purpose of this study was to assess the value of subtraction on post-arterial phase images (*i.e.*, PV, DP/TP and HBP) for the non-invasive diagnosis of HCC in spontaneously hyperintense nodules on T1-weighted images in patients with cirrhosis.

MATERIALS AND METHODS

1. Patients and nodules

This study is a diagnostic accuracy ancillary study of a previously published prospective multicenter study [14,15]. The former study was approved by a National Ethics Committee, registered as NCT00848952, and this ancillary study has been approved by a local ethics committee (registration no. 2021-023). All patients gave written and informed consent.

The initial database included 171 patients with 225 liver nodules. Inclusions were made prospectively between August 2014 and September 2017 in eight university hospital centers across France. Inclusion criteria were: patient with compensated cirrhosis undergoing surveillance with a *de novo* nodule with a diameter ranging between 10 mm and 30 mm, with a maximum of three nodules for each patient. When the patient had more than three nodules, the three largest nodules were selected for further analysis. Exclusion criteria were: nodules located close to or less than 2 cm from a previously treated nodule and previous transarterial chemoembolization. The readings from this database were undertaken by on-site radiologists.

From this initial database with on-site reading, nodules reported to display spontaneous hypersignal when compared to the surrounding liver on pre-contrast T1-weighted images were extracted. Of the 225 nodules (153 HCC) in 171 patients, 55 nodules were reported to show spontaneous hypersignal on T1-weighted images in 45 patients from seven centers. After applying the exclusion criteria, 46 nodules (26 HCC) in 39 patients were analyzed. The flow chart of the study is provided in **Figure 1**.

First, hyperintensity on T1-weighted images was visually confirmed by comparing the nodule to the surrounding liver signal on pre-contrast T1-weighted images by an expert radiologist (AP). Then a centralized reading was made and used for the current study (see below).

2. MRI acquisition protocol

All patients underwent both extracellular (ECA-MRI) and gadoxetate-enhanced (HBA-MRI) MR imaging within one month. MRI examinations were performed at each center, using 1.5-T scanners in seven centers or 3-T scanners in three centers (2 centers used both 3-T and 1.5-T MRI).

The following sequences were acquired: fat-suppressed fast spin-echo T2-weighted imaging; diffusion-weighted imaging (using at least two b-values of 0 and ≥600 s/mm^2); a breath-hold and opposed phase T1-weighted gradient-echo sequence; a fat-suppressed breath-hold imaging T1-weighted gradient-echo sequence with unenhanced, arterial phase (AP), portal venous phase (PVP), delayed phase (DP)/transitional phase (TP) and, for HBA-MRI, hepatobiliary phase (HBP).

AP was acquired 7–8 seconds after the arrival of the contrast agent in the descending aorta, with a single or multi-arterial acquisition; PVP at 70–90 seconds; DP/TP at 3 minutes and HBP at 20 minutes. The contrast agents and saline were injected with a power injector at 2 mL/s for the ECA and 1 mL/s for HBA (Gd-EOB-DTPA, Primovist, Bayer Healthcare, Berlin, Germany).

Subtraction images were obtained for all post-contrast phases (i.e., AP, PVP, DP/TP and HBP). The subtraction images were already present for 31 examinations (out of 70), because they were automatically computed during the MRI examinations as part of

routine clinical practice in the participating centers. These images were therefore used for the centralized readings. For the remaining 39 examinations, the Syngo-via software (*Workstation Syngo-via VB30 Siemens, Erlangen, Germany*) was used to compute post-arterial phase subtraction.

3. Images analysis

Two readers (AP, a senior digestive imaging expert radiologist with seven years of experience, and JB, a junior radiologist, 2 years of residency) independently performed 2 retrospective reviews of each nodule on Synapse (*Synapse V4 Fujifilm PACS*). Readers were blinded from the final diagnosis. Examinations were anonymized and presented in a random fashion.

The first reading session was performed using subtraction images for the arterial phase only (i.e., not for post-arterial phases PVP, DP/TP and HBP), as recommended by guidelines [12,13]. The second reading was performed with all subtraction images (i.e., for AP, PVP, DP/TP and HBP) and at least one month after the first reading in order to avoid recall bias. Where there were discrepancies between the two readings, two additional expert senior radiologists from another tertiary center (MR and RC with 13 years and 5 years of experience, respectively) performed a third reading that included all subtraction images.

Subtraction image quality was assessed using the following scale: no artifacts; mild artifacts but no review limitation; moderate artifacts limiting the review; severe artifacts (unreadable). Imaging features (e.g., non-rim APHE, non-peripheral washout) were reported following the LI-RADS v2018 terminology and definitions [12]. Nodules were therefore classified according to the LI-RADS v2018 and the EASL v2018

recommendations (with ECA and HBA-MRI) and according to KLCA-NCC v2018 and APASL v2018 with HBA-MRI only [1–6].

4. Reference method for diagnosis

The complete reference standard has been described in a previous publication [14]. Briefly, it is based on a step-by-step algorithm built to reach the highest possible specificity and to classify nodules as "HCC" or "not HCC": i) nodules with histology obtained by surgery (resection or transplantation) were classified as "HCC" or "not HCC"; ii) nodules with histology obtained by biopsy were retained only if a diagnosis of tumor (benign or malign) or of cirrhotic nodule (regenerative or dysplastic) was given; iii) if a defined diagnostic of the nodule was not provided by histology, the presence of typical features of HCC using at least two imaging techniques classified the nodule as HCC; iv) a nodule larger than 2 cm associated with an alfa fetoprotein serum level ≥ 200 ng/mL was considered as HCC; v) if the nodule remained negative, the nodule was monitored by imaging and alfa fetoprotein serum level at 3, 6, 9 and 12 months.

5. Statistical analysis

Continuous variables were expressed as mean and ± standard deviation (SD) or median and inter-quartile ranges (Q1, Q3) and ranges when appropriate [16]. Shapiro-Wilk test was used to assess normality. Categorical variables were expressed as raw numbers, proportions and percentages. Due to the small sample size and to limit the potential bias induced by the order in which examinations had been performed, an exact test was used to compare sensitivities and specificities without and with subtraction. The test is formally

equivalent to Fisher's exact test [17]. The resulting *P*-values were adjusted with the Holm procedure for multiplicity issues. The influence of the magnetic field (3T or 1.5T) and the size of the lesion were evaluated through a generalized linear mixed model. All statistical analyses were performed using R version 3.6.0. A *P*-value <0.05 was considered to indicate significant difference.

RESULTS

1. Patients and nodules

A total of 39 patients were ultimately included. There were 35 men and four women, with a mean age of 62 ± 10 (SD) years (range: 46 – 81 years) (**Table I**). The main etiologies of cirrhosis were alcohol abuse (n = 29/39, 74%) and non-alcoholic fatty liver disease (n = 12/39, 31%). Thirty-three patients underwent analyzable ECA-MRI (22 HCCs), and 38 underwent analyzable HBA-MRI (25 HCCs).

Six ECA-MRI (6 nodules), and two HBA-MRI (2 nodules) could not be analyzed because of the impossibility of performing post-hoc subtraction with the Syngo-via software (owing to a different matrix size between pre-contrast and post-contrast sequences). Therefore, ECA-MRI could be analyzed in 33/39 patients (40 nodules, 22 HCC) and HBA-MRI in 37/39 patients (44 nodules, 25 HCC). Out of 46 analyzed lesions 26 were HCC (56%) and the mean tumor size was 17 ± 5 (SD) mm (range: 10 – 30 mm). The flow chart is provided in **Figure 1**. Thirty-two lesions were acquired with a 1.5-T MRI and 14 with a 3-T MRI.

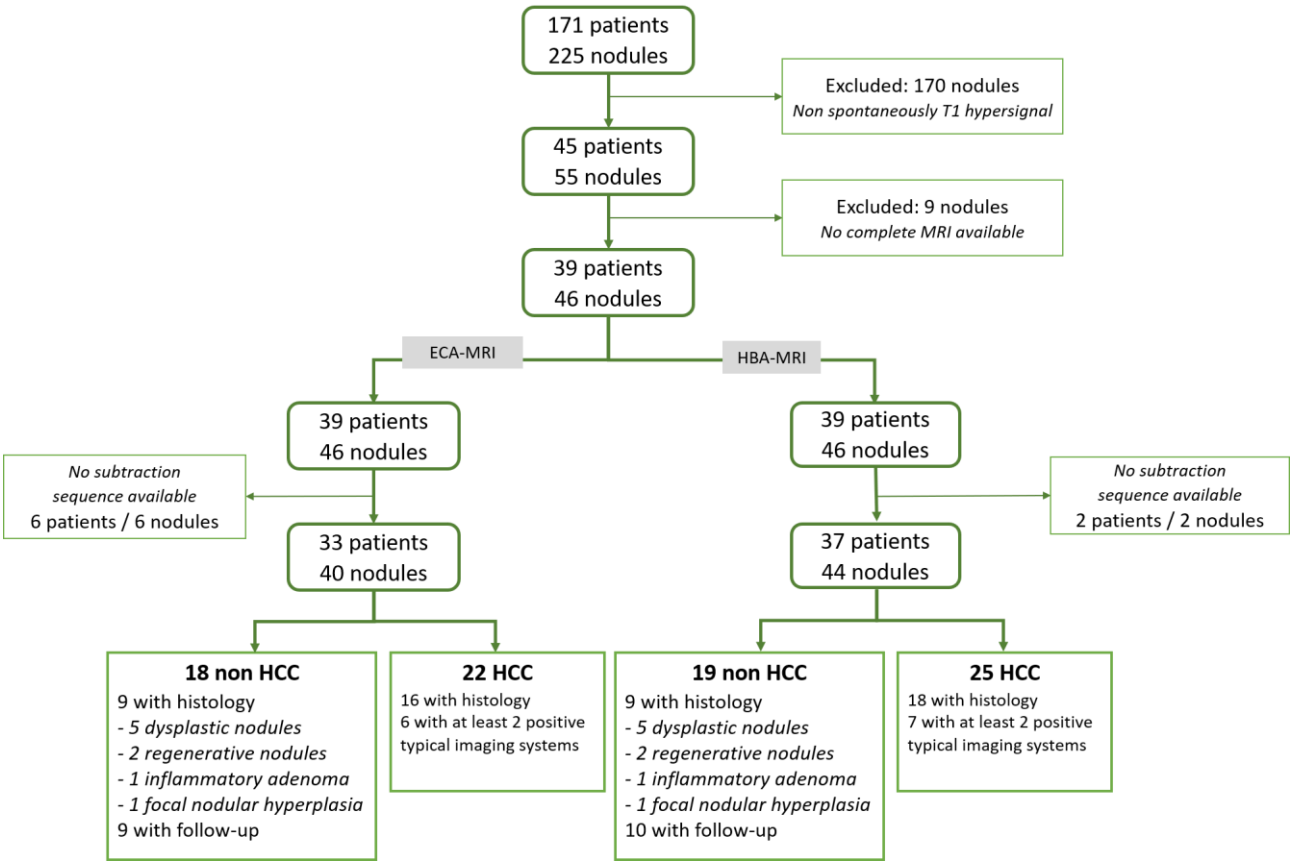

Figure 1 : Study flow chart

Table I: Patient's characteristics

Characteristic	
Sex	
Men (%)	35 (35/39; 90)
Women (%)	4 (4/39; 10)
Age (year)	62 ± 10 [46 - 81]
Etiology of cirrhosis*	
Alcohol	29 (29/39; 74)
HBV	1 (1/39; 3)
HCV	6 (6/39; 15)
NAFLD	12 (12/39; 31)
Hemochromatosis	1 (1/39; 3)
History of HCC	5 (5/39; 13)
Aspartate aminotransferase (IU/L) (n = 38) †	49 [39 - 69]
Alanine aminotransferase (IU/L) (n = 38) †	34 [25 - 54]
Total serum bilirubin (µmol/L) (n = 37) †	21 [15-28]
Albumin (g/L) (n = 36)	34 ± 5 [26 - 45]
Prothrombin time (%) (n = 38)	71 ± 17 [35 - 103]
Platelets (x 10^9/L) (n = 38) †	97 [79 - 133]
Child-Pugh score (n = 36)	
A	25 (25/36; 69)
B	9 (9/36; 25)
C	2 (2/36; 6)
Number of nodules per patient	
1 nodule	33 (33/39; 85)
2 nodules	5 (5/39;13)
3 nodules	1 (1/39; 3)
Size of nodules (mm)	17 ± 5 [10 - 30]
10-19 mm	32 (32/46; 70)
20-30 mm	14 (14/46; 30)

Quantitative data are presented as means ± standard deviations and ranges. Qualitative data are presented as n (proportion; %).
† The mean ± standard deviation is replaced by the median [Q1, Q3] when appropriate for patient characteristics.
*A patient could have multiple etiologies
HBV: hepatitis B virus; HCV: hepatitis C virus; NAFLD: non-alcoholic fatty liver disease

2. Quality of subtraction images

Of the 33 MRI examinations with ECA-MRI, moderate or severe artifacts were present in 4/33 (12%) and 5/32 (16%) subtraction images of PVP and DP, respectively (**Table II**). Of the 37 MRI examinations with HBA-MRI, moderate or severe artifacts were present in 4/37 (11%), 6/36 (17%), and 5/35 (14%) subtraction images of PVP, TP and HBP.

Table II: Quality of subtraction images

Subtraction image quality	**ECA-MRI**			**HBA-MRI**			
	Arterial (n = 33)	PVP (n = 33)	DP (n = 33)	Arterial (n = 37)	PVP (n = 37)	TP (n = 37)	HBP (n = 37)
No artifact	25 (76%)	28 (85%)	24 (73%)	28 (76%)	29 (78%)	25 (68%)	23 (62%)
Mild artifacts	3 (9%)	1 (3%)	3 (9%)	1 (3%)	5 (14%)	6 (16%)	8 (22%)
Moderate artifacts	4 (12%)	4 (12%)	5 (15%)	6 (16%)	3 (8%)	5 (14%)	4 (11%)
Severe artifacts	1 (3%)	0 (0%)	0 (0%)	3 (8%)	1 (3%)	1 (3%)	1 (3%)
No subtraction sequence available	0 (0%)	0 (0%)	1 (3%)	0 (0%)	0 (0%)	1 (3%)	2 (5%)

ECA: extracellular contrast agent; HBA: hepatobiliary contrast agent; PVP: portal venous phase; DP: delayed phase; TP: transitional phase; HBP: hepatobiliary phase.

Data are presented as n (%).

3. Imaging features with and without subtractions on post-arterial phase images

Imaging features without and with the use of subtraction images at AP, PVP, DP/TP and HBP are provided in **Table III**.

On ECA-MRI at PVP, 11/22 (50%) HCCs displayed non-peripheral washout without subtraction compared to 12/22 (55%) when using subtraction ($P > 0.999$). Among the non-HCC cases, non-peripheral washout was present in 2/18 (11%) without subtraction compared to 11/18 (61%) when using subtraction ($P = 0.064$).

On ECA-MRI at DP, 14/22 (64%) HCCs displayed non-peripheral washout compared to 15/22 (68%) when using subtraction. Among the non-HCC nodules, non-peripheral washout was present in 5/18 (28%) without subtraction compared to 12/18 (67%) when using subtraction ($P = 0.069$). On HBA-MRI at HBP, hypointensity was depicted in 12/25 (48%) without subtraction vs. 19/25 (76%) with subtraction ($P = 0.069$).

Using a generalized linear mixed model, there was no influence of the size of the lesion on washout detection for both ECA-MRI and HBA-MRI at PVP and DP/TP (P between 0.068 and 0.544). There was an influence of the magnetic field only for ECA-MRI at PVP ($P = 0.009$).

Table III: Image features with and without subtraction on post-contrast sequences for extracellular (ECA) and hepatobiliary (HBA) MRI contrast agents

		NON-HCC (N = 18 FOR ECA, N = 19 FOR HBA)					
		Nonrim APHE	Non peripheral washout PVP	Non peripheral washout DP	Hyposignal TP	Hyposignal HBP	Enhancing capsule
ECA	No SUB	14 (78%)	2 (11%)	5 (28%)	NA	NA	4 (22%)
	SUB	11 (61%)	11 (61%)	12 (67%)	NA	NA	7 (39%)
HBA	No SUB	16 (84%)	1 (5%)	NA	6 (32%)	8 (42%)	3 (16%)
	SUB	10 (53%)	7 (37%)	NA	11 (58%)	12 (63%)	3 (16%)
		HCC (N = 22 FOR ECA, N = 25 FOR HBA)					
		Nonrim APHE	Non peripheral washout PVP	Non peripheral washout DP	Hyposignal TP	Hyposignal HBP	Enhancing capsule
ECA	No SUB	22 (100%)	11 (50%)	14 (64%)	NA	NA	9 (41%)
	SUB	18 (81%)	12 (55%)	15 (68%)	NA	NA	10 (46%)
HBA	No SUB	25 (100%)	5 (20%)	NA	6 (24%)	12 (48%)	7 (28%)
	SUB	20 (80%)	11 (44%)	NA	15 (60%)	19 (76%)	8 (32%)

Data are presented as n (%).

ECA: extracellular contrast agent; HBA: hepatobiliary contrast agent; HCC: hepatocellular carcinoma; SUB: subtraction; WO: washout; PVP: portal venous phase; DP: delayed phase; TP: transitional phase; HBP: hepatobiliary phase; NA: not applicable

4. Non-invasive diagnosis of HCC with and without subtractions on post-arterial phase images

Details of the diagnostic performance of ECA-MRI and HBA-MRI with and without subtraction images on PVP, DP/TP and HBP images are provided in **Table IV**.

Using LI-RADS v2018, the sensitivity of ECA-MRI for the diagnosis of HCC was 64% (14/22; 95% CI: 41, 83) vs. 73% (16/22; 95% CI: 50, 89) ($P > 0.999$) without and with subtraction images on post-arterial phases, respectively. Corresponding specificity was 67% (12/18; 95% CI: 41, 87) vs. 33% (6/18; 95% CI: 13, 59) ($p = 0.553$), respectively (**Figures 2 and 3**).

The sensitivity of HBA-MRI was 24% (6/25; 95% CI: 9, 45) vs. 44% (11/25; 95% CI: 24, 65) ($P= 0.699$) without and with subtraction images on post-arterial phases, respectively. Corresponding specificity was 95% (18/19; 95% CI: 74, 100) vs. 79% (15/19; 95% CI: 54, 94) ($P = 0.660$), respectively.

Using EASL v2018, the sensitivity of ECA-MRI for the diagnosis of HCC was 59% (13/22; 95% CI: 36, 79) vs. 68% (12/22; 95% CI: 45, 86) ($P > 0.999$) without and with subtraction images on post-arterial phases, respectively. Corresponding specificity was 72% (13/18; 95% CI: 47, 90) vs. 39% (7/18; 95% CI: 17, 64) ($P= 0.553$), respectively.

The sensitivity of HBA-MRI was 16% (4/25; 95% CI: 5, 36) vs. 40.0% (10/25; 95% CI: 21, 61) ($P = 0.628$) without and with subtraction images on post-arterial phases, respectively. Corresponding specificity was 100% (19/19; 95% CI: 82, 100) vs. 79% (15/19; 95% CI: 54, 94) ($P = 0.553$), respectively.

Using KLCA-NCC v2018, the sensitivity of HBA-MRI for the diagnosis of HCC was 68% (17/25; 95% CI: 47, 85) vs. 84% (21/25; 95% CI: 64, 96) ($P = 0.963$) without and with subtraction images on post-arterial phases, respectively. The corresponding specificity was 58% (11/19; 95% CI: 34, 80) vs. 37% (7/19; 95% CI: 16, 62) ($P = 0.660$), respectively.

Using APASL v2017, the sensitivity of HBA-MRI for the diagnosis of HCC was 64% (16/25; 95% CI: 43, 82) vs. 84% (21/25; 95% CI: 64, 96) (*P* = 0.785) without and with subtraction images on post-arterial phases, respectively. The corresponding specificity was 63% (12/19; 95% CI: 38, 84) vs. 37% (7/19; 95% CI: 16, 62) (*P* = 0.582), respectively.

Table IV: Performance of ECA-MRI and HBA-MRI without and with subtraction on post-arterial phase images according to LI-RADS v2018, EASL v2018, KLCA-NCC v2018, APASL v2017

Guideline	HCC	Se	Spe	NPV	PPV	DA	False positive
LI-RADS ECA (n = 40)	22	64 (14/22; 41, 83)	67 (12/18; 41, 87)	60 (12/20; 36, 81)	70 (14/20; 46, 88)	65 (26/40; 48, 79)	6 (3 with histology: 2 regenerative nodules; 1 dysplastic nodule)
LI-RADS sub ECA (n = 40)	22	73 (16/22; 50, 89)	33 (6/18; 13, 59)	50 (6/12; 21, 79)	57 (16/28; 37, 76)	55 (22/40; 39, 71)	12 (6 with histology: 2 regenerative nodules; 2 dysplastic nodules; 1 adenoma; 1 nodular focal hyperplasia)
*P**		1	0.553				
LI-RADS HBA (n = 44)	25	24 (6/25; 9, 45)	95 (18/19; 74, 100)	49 (18/37; 32, 66)	86 (6/7; 42, 100)	55 (24/44; 39, 70)	1 (1 with histology: 1 dysplastic nodule)
LI-RADS sub HBA (n = 44)	25	44 (11/25; 24, 65)	79 (15/19; 54, 94)	52 (15/29; 33, 71)	73 (11/15; 45, 92)	59 (26/44; 43, 74)	4 (2 with histology: 2 dysplastic nodules)
*P**		0.699	0.660				
EASL ECA (n = 40)	22	59 (13/22; 36, 79)	72 (13/18; 47, 90)	59 (13/22; 36, 79)	72 (13/18; 47, 90)	65 (26/40; 48, 79)	5 (2 with histology: 2 regenerative nodules)
EASL sub ECA (n = 40)	22	68 (12/22; 45, 86)	39 (7/18; 17, 64)	50 (7/14; 23, 77)	58 (15/26; 37, 77)	55 (22/40; 39, 71)	11 (6 with histology: 2 regenerative nodules; 2 dysplastic nodules; 1 focal nodular hyperplasia; 1 adenoma)
*P**		1	0.553				
EASL HBA (n = 44)	25	16 (4/25; 5, 36)	100 (19/19; 82, 100)	48 (19/40; 32, 64)	100 (4/4; 40, 100)	52 (23/44; 37, 68)	0
EASL sub HBA (n = 44)	25	40 (10/25; 21, 61)	79 (15/19; 54, 94)	50 (15/30; 31, 69)	71 (10/14; 42, 92)	57 (25/44; 41, 72)	4 (2 with histology: 2 dysplastic nodules)
*P**		0.682	0.553				

KLCA-NCC HBA (n = 44)	25	68 (17/25; 47, 85)	58 (11/19; 34, 80)	58 (11/19; 34, 80)	68 (17/25; 47, 85)	64 (28/44; 48, 78)	8 (6 with histology: 3 dysplastic nodules; 1 adenoma; 2 regenerative nodules)
KLCA-NCC HBA sub (n = 44)	25	84 (21/25; 64, 96)	37 (7/19; 16, 61)	64 (7/11; 31, 89)	64 (21/33; 45, 80)	64 (28/44; 48, 78)	12 (7 with histology: 4 dysplastic nodules; 1 adenoma; 2 regenerative nodules)
*P**		0.963	0.660				
APASL HBA (n = 44)	25	64 (16/25; 43, 82)	63 (12/19; 38, 84)	57 (12/21; 34, 78)	70 (16/23; 47, 87)	64 (28/44; 48, 78)	7 (5 with histology: 3 dysplastic nodules; 1 adenoma; 1 regenerative nodule)
APASL HBA sub (n = 44)	25	84 (21/25; 64, 96)	37 (7/19; 16, 62)	64 (7/11; 31, 89)	64 (21/33; 45, 80)	64 (28/44; 48, 78)	12 (7 with histology: 4 dysplastic nodules; 1 adenoma; 2 regenerative nodules)
*P**		0.785	0.582				

ECA: extracellular contrast agent; HBA: hepatobiliary contrast agent; HCC: hepatocellular carcinoma; sub: subtraction

Se: sensitivity; Spe: specificity; NPV: negative predictive value; PPV: positive predictive value: DA: diagnostic accuracy

Data are presented in % (proportion, 95% CI).

* Without subtraction vs. with subtraction using Fisher tests adjusted with Holm correction for multiple testing.

Post-arterial phase corresponds to portal venous phase, delayed phase, transitional phase and hepatobiliary phase.

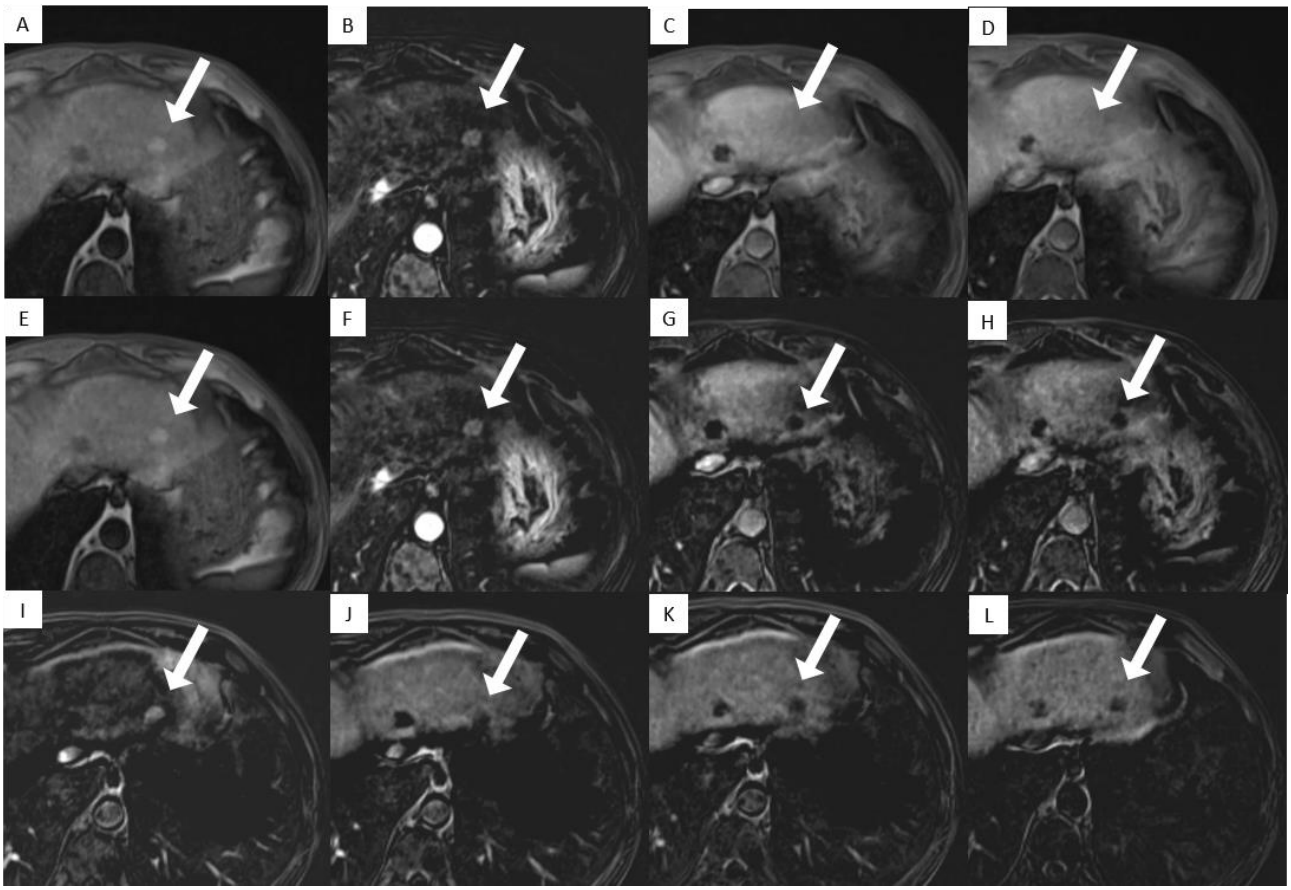

Figure 2. 46-year-old man with alcoholic cirrhosis. A and E. Unenhanced T1-weighted MR image in the axial plane shows spontaneously hyperintense nodule in segment II (arrow). B and F. T1-weighted MR image at arterial phase after intra-venous injection of extracellular contrast agent shows arterial phase hyperenhancement on subtraction. C. Portal venous and D. Delayed phase shows iso signal. G and H. Subtracted T1-weighted MR images at portal venous (G) and delayed (H) phases show washout. I. T1-weighted MR image at arterial phase after intra-venous injection of hepatobiliary contrast agent shows arterial phase hyperenhancement on subtraction. J, K and L. Subtracted T1-weighted MR image after intra-venous contrast show washout at portal venous (J) and transitional (K) and hepatobiliary (L) phases. The lesion was classified LIRADS 3 and non-hepatocellular carcinoma according to EASL v2018 without subtraction and LIRADS 5 and hepatocellular carcinoma according to EASL v2018 with subtraction. The final diagnosis in histology was inflammatory adenoma.

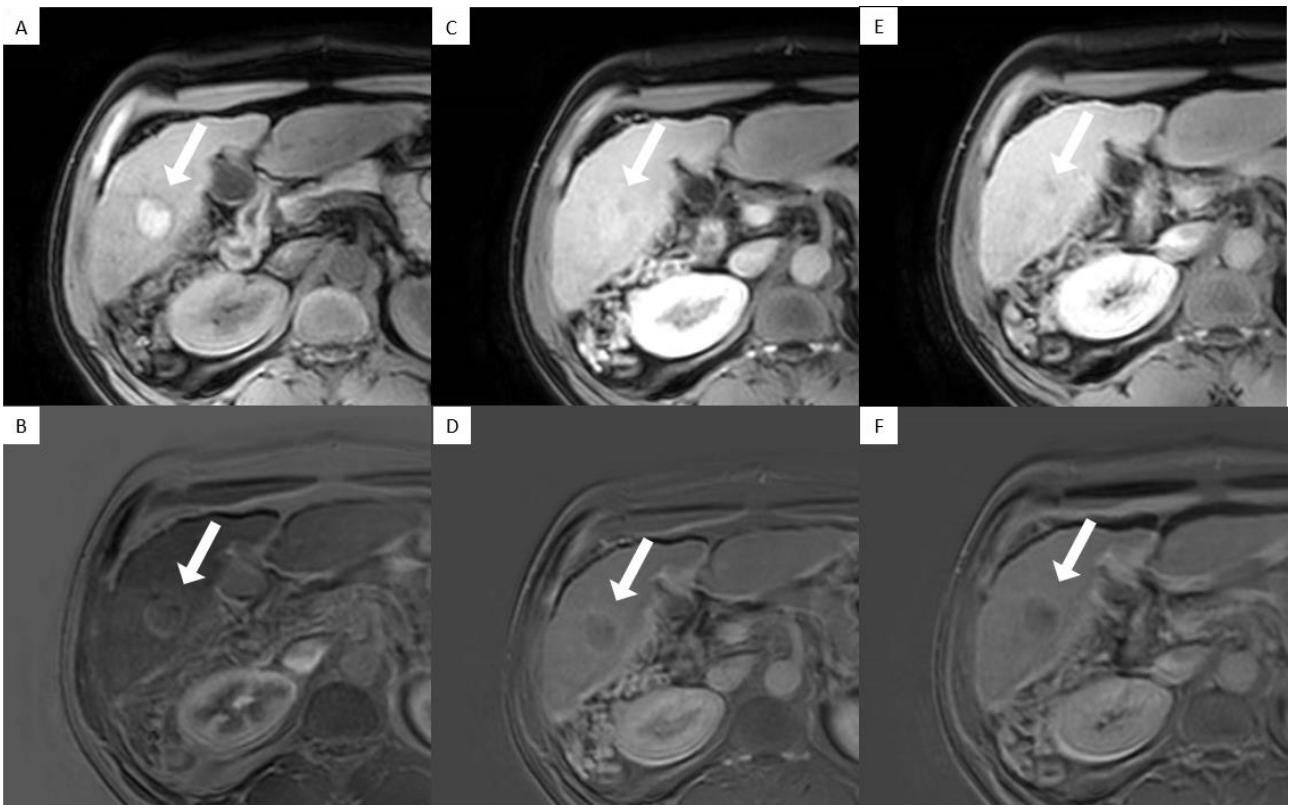

Figure 3. 49-year-old man with ethylic cirrhosis and prior history of hepatocellular carcinoma. A. Unenhanced T1-weighted MR image in the axial plane shows spontaneously hyperintense nodule in segment V. B. T1-weighted MR image at arterial phase after intra-venous contrast of hepatobiliary contrast agent shows subtle arterial phase hyperenhancement on subtraction images. C. T1-weighted MR image at portal venous phase shows a slight hyperintensity. D. Subtracted T1-weighted MR image at portal venous phase shows both capsule and washout. E. T1-weighted MR image at transitional phase shows possible slight hyposignal. F. Subtracted T1-weighted MR image at transitional phase shows capsule again. The lesion was classified LIRADS 4 and non-hepatocellular carcinoma according to EASL v2018 without subtraction and LIRADS 5 and HCC using subtraction. The final diagnosis (histology) was hepatocellular carcinoma.

DISCUSSION AND CONCLUSION

This study shows that using subtraction on post-arterial phase images decreases the specificity of MRI for the non-invasive diagnosis of HCC in spontaneously hyperintense nodules on T1-weighted images developed on cirrhosis. When using the LI-RADS v2018, the specificity decreased from 67% to 33% with ECA-MRI and from 95% to 79% with HBA-MRI. This marked decrease was primarily due to the depiction of more non-peripheral washout in non-HCC lesions (e.g., dysplastic nodules, adenoma) with subtraction images (**Figure 2**).

Our results suggest that subtraction images on post-arterial phases in the subset of HCCs do not represent added value. Indeed, the rate of washout depiction was not modified by subtraction imaging, suggesting that native images are sufficient. The use of subtraction on PVP for the non-invasive diagnosis of HCC with HBA-MRI has been evaluated in a prior study by Chung et al. [18]. The authors suggested that image subtraction on portal venous phase may upgrade the LI-RADS categories because of its superior ability to depict an enhancing capsule and its incremental benefit in showing washout. The inclusion of different populations of tumors can explain this discrepancy with our results. While we focused on spontaneously hyperintense nodules on T1-weighted images, only five out of 120 included HCCs in the study by Chung et al. displayed hyperintensity on T1-weighted images. Notably, the results of both studies are consistent concerning the depiction of an enhancing capsule. However, the number of LI-RADS category upgrades in our study remained low (from LR-4 to LR-5 for two HCCs, **Figure 3**) because of the limited value of the enhancing capsule, as suggested by Cannella et al. [19].

Arterial subtraction images have been shown to significantly improve the sensitivity of early-stage HCC diagnosis without a significant decrease in specificity [13,20,21], thus justifying its endorsement by the main guidelines, especially the LI-RADS [2,3]. One may therefore wonder why similar results are not replicated with the washout. As already mentioned, the definition

of imaging features is purely visual [22]. Several studies have consistently shown that the inter-reader agreement is better for APHE than for washout [23,24]. One part of an explanation may be the difference in contrast between the liver and the tumors in different phases. Using a quantitative approach, Liu et al. showed that the difference in attenuation between hepatic tumors (both HCC and non-HCC) and the liver was significantly higher in the arterial phase compared to the portal venous or delayed phases [25]. This was confirmed by Kloeckner et al. [26] and Pfeiffer et al. [27]. One may therefore hypothesize that the marked difference in attenuation on arterial phase due to tumor neoangiogenesis is accurately captured by subtraction imaging. Conversely, minimal differences in attenuation on portal venous or delayed phases that may not be visually identified as washout *per se* may be artificially increased by the image subtraction process. According to this perspective, subtraction images on post-arterial phases would depict washout that may not necessarily reflect tumor composition or structure but rather be a by-product of image post-processing.

One further explanation is the existence of motion artifacts due to the movements of the liver between the different breath-hold acquisitions. The quality of subtraction images is therefore related to the size of the lesions and is reduced in tumors smaller than 2 cm [9]. This may be improved by using registration methods on PVP, DP/TP or HBP images, or by the recent development of free-breathing T1 imaging, with acquisition performed in one continuous run with golden-angle radial sparse parallel, leading to artifact-free images [28].

Our study comes with certain limitations. First, while the data are derived from prospective studies, the current study is retrospective. Second, we focused on nodules hyperintense on T1-weighted images, limiting the study population to 46. This was intentional, as subtraction imaging on the arterial phase is recommenced in these nodules only. The extent to which a broader application of subtraction images may be beneficial remains to be analyzed in future studies. Third, no manual or computer-guided registration was performed before subtraction.

This may have decreased the image quality on a subset of tumors, but it represents a real-life setting. Finally, the influence of several factors, such as location, heterogeneity or influence of the presence of blood products, has not been evaluated.

In conclusion, the results of our study suggest that the use of subtraction images on post-arterial phases (*i.e.*, PVP, DP/TP and HBP) is not relevant for the non-invasive diagnosis of HCC in spontaneously hyperintense nodules on T1-weighted images in patients with cirrhosis.

REFERENCES

[1] Galle PR, Forner A, Llovet JM, Mazzaferro V, Piscaglia F, Raoul J-L, et al. EASL Clinical Practice Guidelines: Management of hepatocellular carcinoma. J Hepatol 2018;69:182–236.

[2] Chernyak V, Fowler KJ, Kamaya A, Kielar AZ, Elsayes KM, Bashir MR, et al. Liver Imaging Reporting and Data System (LI-RADS) Version 2018: Imaging of Hepatocellular Carcinoma in At-Risk Patients. Radiology 2018;289:816–30.

[3] Abdelrahman AS, Ekladious MEY, Badran EM, Madkour SS. Liver imaging reporting and data system (LI-RADS) v2018: Reliability and agreement for assessing hepatocellular carcinoma locoregional treatment response. Diagn Interv Imaging 2022;103:524–34.

[4] Korean Liver Cancer Association (KLCA), National Cancer Center (NCC), Goyang, Korea. 2018 Korean Liver Cancer Association–National Cancer Center Korea Practice Guidelines for the Management of Hepatocellular Carcinoma. Korean J Radiol 2019;20:1042.

[5] Kudo M, Matsui O, Izumi N, Iijima H, Kadoya M, Imai Y, et al. JSH Consensus-Based Clinical Practice Guidelines for the Management of Hepatocellular Carcinoma: 2014 Update by the Liver Cancer Study Group of Japan. Liver Cancer 2014;3:458–68.

[6] Omata M, Cheng A-L, Kokudo N, Kudo M, Lee JM, Jia J, et al. Asia–Pacific clinical practice guidelines on the management of hepatocellular carcinoma: a 2017 update. Hepatol Int 2017;11:317–70.

[7] Rimola J, Forner A, Tremosini S, Reig M, Vilana R, Bianchi L, et al. Non-invasive diagnosis of hepatocellular carcinoma ⩽2cm in cirrhosis. Diagnostic accuracy assessing fat, capsule and signal intensity at dynamic MRI. J Hepatol 2012;56:1317–23.

[8] Shimizu A, Ito K, Sasaki K, Hayashida M, Tanabe M, Shimizu K, et al. Small hyperintense hepatic lesions on T1-weighted images in patients with cirrhosis: evaluation with serial MRI and imaging features for clinical benignity. Magn Reson Imaging 2007;25:1430–6.

[9] Yu J-S, Kim YH, Rofsky NM. Dynamic Subtraction Magnetic Resonance Imaging of Cirrhotic Liver: Assessment of High Signal Intensity Lesions on Nonenhanced T1-Weighted Images. J Comput Assist Tomogr 2005;29:51–8.

[10] Furlan A, Marin D, Bae KT, Lagalla R, Agnello F, Bazzocchi M, et al. Focal Liver Lesions Hyperintense on T1-Weighted Magnetic Resonance Images. Semin Ultrasound CT MRI 2009;30:436–49.

[11] Chou C-T. Differentiation between dysplastic nodule and early-stage hepatocellular carcinoma: The utility of conventional MR imaging. World J Gastroenterol 2013;19:7433.

[12] Kambadakone AR, Fung A, Gupta RT, Hope TA, Fowler KJ, Lyshchik A, et al. LI-RADS technical requirements for CT, MRI, and contrast-enhanced ultrasound. Abdom Radiol 2018;43:56–74.

[13] An C, Park M-S, Kim D, Kim Y-E, Chung W-S, Rhee H, et al. Added value of subtraction imaging in detecting arterial enhancement in small (<3 cm) hepatic nodules on dynamic contrast-enhanced MRI in patients at high risk of hepatocellular carcinoma. Eur Radiol 2013;23:924–30.

[14] Paisant A, Vilgrain V, Riou J, Oberti F, Sutter O, Laurent V, et al. Comparison of extracellular and hepatobiliary MR contrast agents for the diagnosis of small HCCs. J Hepatol 2020;72:937–45.

[15] Paisant A, Gillard M, Oberti F, Roux M, Aubé C. Validation of a Diagnostic Algorithm for Hepatocellular Carcinoma at Gadoxetic Acid–enhanced MRI. Radiology 2021;300:184–6.

[16] Barat M, Jannot A-S, Dohan A, Soyer P. How to report and compare quantitative variables in a radiology article. Diagn Interv Imaging 2022;103:571–3.

[17] Gart JJ. An exact test for comparing matched proportions in crossover designs. Biometrika 1969;56:75–80.

[18] Chung JW, Yu J-S, Choi JM, Cho E-S, Kim JH, Chung J-J. Subtraction Images From Portal Venous Phase Gadoxetic Acid–Enhanced MRI for Observing Washout and Enhancing Capsule Features in LI-RADS Version 2018. Am J Roentgenol 2020;214:72–80.

[19] Cannella R, Ronot M, Sartoris R, Cauchy F, Hobeika C, Beaufrere A, et al. Enhancing capsule in hepatocellular carcinoma: intra-individual comparison between CT and MRI with extracellular contrast agent. Diagn Interv Imaging 2021;102:735–42.

[20] Kim DH, Choi SH, Byun JH, Kang JH, Lim Y-S, Lee SJ, et al. Arterial subtraction images of gadoxetate-enhanced MRI improve diagnosis of early-stage hepatocellular carcinoma. J Hepatol 2019;71:534–42.

[21] Choi SH, Kim SY, Lee SS, Shim JH, Byun JH, Baek S, et al. Subtraction Images of Gadoxetic Acid–Enhanced MRI: Effect on the Diagnostic Performance for Focal Hepatic Lesions in Patients at Risk for Hepatocellular Carcinoma. Am J Roentgenol 2017;209:584–91.

[22] Fowler KJ, Bashir MR, Fetzer DT, Kitao A, Lee JM, Jiang H, et al. Universal Liver Imaging Lexicon: Imaging Atlas for Research and Clinical Practice. RadioGraphics 2023;43:e220066.

[23] Davenport MS, Khalatbari S, Liu PSC, Maturen KE, Kaza RK, Wasnik AP, et al. Repeatability of Diagnostic Features and Scoring Systems for Hepatocellular Carcinoma by Using MR Imaging. Radiology 2014;272:132–42.

[24] Rimola J, Sapena V, Brancatelli G, Darnell A, Forzenigo L, Mähringer-Kunz A, et al. Reliability of extracellular contrast versus gadoxetic acid in assessing small liver lesions using liver imaging reporting and data system v.2018 and European association for the study of the liver criteria. Hepatology 2022;76:1318–28.

[25] Liu YI, Shin LK, Jeffrey RB, Kamaya A. Quantitatively Defining Washout in Hepatocellular Carcinoma. Am J Roentgenol 2013;200:84–9.

[26] Kloeckner R, Pinto dos Santos D, Kreitner K-F, Leicher-Düber A, Weinmann A, Mittler J, et al. Quantitative assessment of washout in hepatocellular carcinoma using MRI. BMC Cancer 2016;16:758.

[27] Pfeiffer D, Parakh A, Patino M, Kambadakone A, Rummeny EJ, Sahani DV. Iodine material density images in dual-energy CT: quantification of contrast uptake and washout in HCC. Abdom Radiol 2018;43:3317–23.

[28] Yoon JH, Nickel MD, Peeters JM, Lee JM. Rapid Imaging: Recent Advances in Abdominal MRI for Reducing Acquisition Time and Its Clinical Applications. Korean J Radiol 2019;20:1597.

FIGURES

TABLES

TABLE OF CONTENTS

BIZEUL Jocelyn

Evaluation du lavage en IRM avec soustraction dans le diagnostic de carcinome hépatocellulaire parmi les nodules en hypersignal T1 spontané chez les patients cirrhotiques

RÉSUMÉ

Introduction : le but de cette étude était d'évaluer l'intérêt de la soustraction sur les images des phases post-artérielles (c'est-à-dire les phases veineuse portale, tardive/transitionnelle et hépatobiliaire) pour le diagnostic non invasif du carcinome hépatocellulaire (CHC) parmi les nodules spontanément hyperintenses sur l'imagerie pondérée en T1 chez les patients atteints de cirrhose.

Matériels et méthodes : quarante-cinq patients présentant un total de 55 nodules hépatiques spontanément hyperintenses sur les images pondérées en T1 ont été initialement retenus. Tous les patients ont subi une IRM hépatique en utilisant un agent extracellulaire. La sensibilité et la spécificité de chaque nodule ont été évaluées à l'aide du LI-RADS (Liver Imaging Reporting and Data System) au cours de deux séances de lecture réalisées d'abord sans puis avec des images de soustraction sur les images en phase post-artérielle. Le gold standard final a été défini par un algorithme précédemment publié combinant l'histologie, l'imagerie typique, l'alfa foetoprotéine et le suivi.

Résultats : quarante-six nodules (26 CHC) chez 39 patients atteints de cirrhose ont été analysés. En utilisant le LI-RADS, la sensibilité et la spécificité pour le diagnostic de CHC étaient de 64 % (IC 95 % : 41, 83) et 67 % (IC 95 % : 41, 87) sans images de soustraction ; et de 73 % (IC 95 % : 50, 89) (P = 1,000) et 33 % (IC 95 % : 13, 59) (P = 0,553) sur les images de soustraction utilisant un agent de contraste extracellulaire. Cinquante-cinq pour cent (22/40) des nodules présentaient un lavage sans soustraction et 70 % (28/40) sur les images de soustraction obtenues avec un agent de contraste extracellulaire. Vingt nodules sur 40 (50%) ont été classés LI-RADS 5 sans soustraction, et 28 nodules sur 40 (70%) avec soustraction.

Conclusion : ces résultats suggèrent que l'utilisation d'images de soustraction sur les images de la phase post-artérielle (c'est-à-dire PVP, DP/TP et HBP) n'est pas pertinente pour le diagnostic non invasif du CHC pour les nodules spontanément hyperintenses sur les images pondérées en T1 chez les patients atteints de cirrhose hépatique.

Mots-clés : Carcinome hépato-cellulaire, Imagerie par résonnance magnétique, Soustraction

Evaluation of washout using image subtraction for the diagnosis of hepatocellular carcinoma in cirrhotic patients with native T1-hyperintense nodules

ABSTRACT

Purpose : the purpose of this study was to assess the value of subtraction on post-arterial phase images (i.e., portal venous, delayed/transitional and hepatobiliary phases) for the non-invasive diagnosis of hepatocellular carcinoma (HCC) in spontaneously hyperintense nodules on T1-weighted imaging in patients with cirrhosis.

Materials and methods : forty-five patients with a total 55 hepatic nodules that were spontaneously hyperintense on T1-weighted images were initially retrieved. All patients underwent MRI examination of the liver using extracellular agent. Each nodule was assessed for sensitivity and specificity using LI-RADS (Liver Imaging Reporting and Data System) during two reading sessions performed first without then with subtraction images on post-arterial phase images. The final gold standard was defined by a step-by-step algorithm previously published combining histology, typical imaging, alfa fetoprotein and follow-up.

Results : Forty-six nodules (26 HCC) in 39 patients with cirrhosis were analyzed. Using LI-RADS, the sensitivity and specificity for the diagnosis of HCC were 64% (95% CI: 41, 83) and 67% (95% CI: 41, 87) without subtraction images; and 73% (95%CI: 50, 89) (P = 1.000) and 33% (95%CI: 13, 59) (P = 0.553) on subtraction images using extracellular contrast agent. Fifty-five percent (22/40) of nodules displayed a washout without subtraction and 70% (28/40) did so on subtraction images obtained with extracellular contrast agent. Twenty nodules out of 40 (50%) were classified LI-RADS 5 without subtraction, and 28 out of 40 nodules (70%) with subtraction.

Conclusion : These results suggest that the use of subtraction images on post-arterial phase images (i.e., PVP, DP/TP and HBP) is not relevant for the non-invasive diagnosis of HCC for spontaneously hyperintense nodules on T1-weighted images in patients with liver cirrhosis.

Keywords : Hepatocellular Carcinoma, Magnetic Resonance Imaging, Subtraction Technique

FACULTÉ DE SANTÉ
UNIVERSITÉ D'ANGERS